

Ascertaining higher-order quantum correlations in high energy physics

Ao-Xiang Liu¹ and Cong-Feng Qiao^{1, 2, *}

¹*School of Physical Sciences, University of Chinese Academy of Sciences, 1 Yanqihe East Rd, Beijing 101408, China*

²*ICTP-AP, University of Chinese Academy of Sciences, Beijing 100190, China*

(Dated: January 15, 2026)

Nonlocality is a peculiar nature of quanta and it stands as an important quantum resource in application. Yet mere linear property of it, viz. the first order in moment, has been explored through various inequalities. Noticing the vast higher-order regime unexplored, in this study we investigate the higher-order quantum correlations in entangled hyperon-antihyperon system, which may be generated massively in charmonium decays. A new type of Clauser-Horne inequality for statistical cumulants and central moments is formulated. We find that a significant violation of the third-order constraint, indicating the existence of higher-order correlation, exists in hyperon-antihyperon system and can be observed in high energy physics experiments, like BESIII and Belle II. Notably, the violation manifests more in higher energy systems of the $\Lambda\bar{\Lambda}$ pair against the kinematic contamination of timelike events.

I. INTRODUCTION

In their seminal 1935 paper [1], Einstein, Podolsky, and Rosen (EPR) exposed the fundamental conflict between the assumptions of local realism and the completeness of the quantum mechanical description. This conceptual debate was transformed into a testable physical question by Bell, whose theorem provided a strict boundary between local hidden variable (LHV) theories and quantum mechanics [2]. Since then, a rich hierarchy of EPR correlations, including entanglement, steering, and Bell nonlocality, has been established [3–8], all of which are recognized as essential resources for quantum information processing [9–11]. While experiments with photons have effectively ruled out LHV models [4–6, 12–16], the verification of these fundamental principles using entangled massive particles at colliders remains a nascent frontier [17–23].

Verifying these principles in high-energy physics faces inherent challenges. High-energy decays are passive processes lacking active control over measurement settings [24], and the absence of direct dichotomic observables complicates standard correlation functions [25]. Furthermore, Bell tests using Clauser-Horne-Shimony-Holt (CHSH) inequalities often suffer from the “loophole” induced by data renormalization [26]. Recently, the generalized Clauser-Horne (CH) inequality [27] addressed this renormalization issue by modeling hyperon weak decay within a generalized positive operator-valued measure (POVM) framework, which has been experimentally implemented in hyperon-antihyperon systems at BESIII [28].

These tests remain limited by their reliance on first-order statistical moments (expectation values). The complete statistical information of a quantum measurement is, however, not fully captured by its mean. While the linear regime has been extensively explored through var-

ious inequalities, the higher-order regime remains virtually unexplored. Recent theoretical advances highlight that higher-order quantum correlations constitute a distinct quantum resource, potentially revealing nonlocal phenomena fundamentally different from standard Bell nonlocality [29]. However, despite these insights, the experimental verification of such quantum correlations stays uncharted.

This deficiency is addressed in the present work by formulating a test of higher-order quantum correlations in entangled hyperon-antihyperon system. The focus is placed on the weak decays of entangled hyperon-antihyperon pairs produced in charmonium decays ($\chi_{c0}, \eta_c \rightarrow \Lambda\bar{\Lambda}$ and $J/\psi \rightarrow Y\bar{Y}$), where the hyperon weak decay functions as a self-analyzing polarimeter and is treated within the generalized POVM framework to account for decay parameters. Specifically, a hierarchy of criteria is derived, starting with the generalized CH inequality based on the second-order cumulant and extending to the third-order skewness constraint. The analysis reveals that the hyperon-antihyperon system exhibits a significant violation of this third-order constraint, serving as a signature of higher-order quantum correlations that is observable in high energy physics experiments like BESIII and Belle II. To ensure the validity of these tests in realistic collider environments, these algebraic bounds are rigorously modified to account for the unavoidable timelike separated background, a correction that confirms the specific robustness of nonlocality violations in the $\chi_{c0} \rightarrow \Lambda\bar{\Lambda}$ channel. Furthermore, the analysis is extended to the fourth-order central moment. Its possible connection to state-independent contextuality is briefly discussed as a potential avenue for future investigation.

II. PRELIMINARIES

Consider a quantum measurement described by a collection of measurement operators $\{M_m\}$ performed on a system in the state $|\psi\rangle$. The probability of obtaining the m -th outcome is given by $p_m = \langle\psi|E_m|\psi\rangle$, where

* qiaocf@ucas.ac.cn

$E_m = M_m^\dagger M_m$ are positive operators satisfying the completeness relation $\sum_m E_m = I$.

For a qubit (or spin-1/2) system, the measurement M_m is typically implemented by an apparatus aligned along a direction \mathbf{n} , where each particle triggering the apparatus yields one of the dichotomic outcomes labeled \pm . The general POVM operators for such a system can be parametrized as:

$$E_{\pm}(\mathbf{a}) \equiv \frac{\xi^{(\pm)} \pm \alpha \boldsymbol{\sigma} \cdot \mathbf{a}}{2}. \quad (1)$$

Here, $\boldsymbol{\sigma} = (\sigma_x, \sigma_y, \sigma_z)$ is the vector of Pauli matrices. The parameters $\xi^{(\pm)}$ and α characterize the degrees of bias and unsharpness, respectively, defined by $\xi^{(\pm)} = 1 \pm \eta$ with the constraint $|\eta \pm \alpha| \leq 1$. The general POVM in Eq. (1) reduces to the projective measurement when $\eta = 0$, $|\alpha| = 1$. Focusing on the “+” outcome, the probability of observing + upon measuring along direction \mathbf{a} is

$$P_+(\mathbf{a}) \equiv \langle \psi | E_+(\mathbf{a}) | \psi \rangle. \quad (2)$$

In an LHV theory, the measurement statistics are governed by a hidden parameter λ . In a bipartite system, the local observables X, Y measured on subsystems A, B are predetermined by hidden variable λ as $X(\lambda), Y(\lambda)$. For a function $\mathcal{S}(X, Y)$ of local observables, its expectation value is given by:

$$\langle \mathcal{S} \rangle_{\text{LHV}} = \int \mathcal{S}(X(\lambda), Y(\lambda)) \rho(\lambda) d\lambda, \quad (3)$$

where $\rho(\lambda)$ is the normalized probability distribution of the hidden variable λ . According to Eq. (3), the probability of obtaining a specific outcome in the LHV framework is:

$$P_{\pm}(\mathbf{n}) = \int P_{\pm}(\mathbf{n}, \lambda) \rho(\lambda) d\lambda, \quad (4)$$

where $P_{\pm}(\mathbf{n}, \lambda) \in [\frac{1 \pm \eta - |\alpha|}{2}, \frac{1 \pm \eta + |\alpha|}{2}]$ represents the probability of the ± 1 outcome conditioned on λ , bounded by the eigenvalues of the POVM operator. For a bipartite system composed of subsystems A and B , the joint probability of outcomes j and k (with $j, k \in \{+, -\}$) along measurement directions \mathbf{a} and \mathbf{b} is:

$$P_{jk}(\mathbf{a}, \mathbf{b}) = \int P_j(\mathbf{a}, \lambda) P_k(\mathbf{b}, \lambda) \rho(\lambda) d\lambda. \quad (5)$$

Let us define the generalized Clauser-Horne (CH) functional for a bipartite system as follows:

$$\begin{aligned} \mathbf{B}_{\text{CH}}^{jk} \equiv & P_{jk}(\mathbf{a}, \mathbf{b}) - P_{jk}(\mathbf{a}, \mathbf{b}') + P_{jk}(\mathbf{a}', \mathbf{b}) + P_{jk}(\mathbf{a}', \mathbf{b}') \\ & - (1 + k\eta_b) P_j(\mathbf{a}') - (1 + j\eta_a) P_k(\mathbf{b}) \\ & + \frac{(1 + j\eta_a)(1 + k\eta_b) - |\alpha_a \alpha_b|}{2}. \end{aligned} \quad (6)$$

Here, $\eta_{a,b}$ and $\alpha_{a,b}$ are the bias and unsharpness parameters for subsystems A and B , respectively. Without loss

of generality, we set $j = k = +$ and omit the outcome superscripts in the subsequent analysis.

In quantum mechanics, the joint probability for a bipartite state ρ is predicted by:

$$P_{jk}(\mathbf{a}, \mathbf{b}) = \text{Tr} [\rho E_j(\mathbf{a}) \otimes E_k(\mathbf{b})]. \quad (7)$$

Consequently, the operator form of \mathbf{B}_{CH} in Eq. (20) may be defined as the expectation value of the following operator:

$$\begin{aligned} \mathbf{B}_{\text{CH}} \equiv & E_+(\mathbf{a}) \otimes E_+(\mathbf{b}) - E_+(\mathbf{a}) \otimes E_+(\mathbf{b}') \\ & + E_+(\mathbf{a}') \otimes E_+(\mathbf{b}) + E_+(\mathbf{a}') \otimes E_+(\mathbf{b}') \\ & - (1 + \eta_b) E_+(\mathbf{a}') \otimes I - (1 + \eta_a) I \otimes E_+(\mathbf{b}) \\ & + \frac{(1 + \eta_a)(1 + \eta_b) - |\alpha_a \alpha_b|}{2} I \otimes I. \end{aligned} \quad (8)$$

The expectation value of \mathbf{B}_{CH} predicted by quantum theory is thus:

$$\mathbf{B}_{\text{CH}} = \langle \mathbf{B}_{\text{CH}} \rangle = \text{Tr} (\rho \mathbf{B}_{\text{CH}}). \quad (9)$$

For simplicity, the representative orthogonal measurement configuration $(\mathbf{a} \perp \mathbf{a}', \mathbf{b} \perp \mathbf{b}')$ is adopted in this work, which is known to be optimal for revealing quantum nonlocality in spin-correlated systems [30, 31].

III. HIGHER-ORDER QUANTUM CORRELATIONS VIA CUMULANTS AND CENTRAL MOMENTS

Standard Bell tests verify quantum nonlocality by constraining the first moment (mean value) of a Bell operator. However, the probability distribution of quantum measurement outcomes contains a complete hierarchy of statistical information that is often discarded in first-order tests. In this section, a theoretical framework that exploits this discarded information is established.

A. Statistical Moments and Cumulants

Given a random variable X , the moment generating function takes the following form

$$\langle e^{sX} \rangle = \sum_{n=0}^{\infty} \langle X^n \rangle \frac{s^n}{n!}, \quad s \in \mathbb{C}. \quad (10)$$

Here, the parameter s is a complex number. Taking the natural logarithm of both sides of Eq. (10), one obtains the cumulant generating function:

$$K(s) = \ln \langle e^{sX} \rangle = \sum_{n=1}^{\infty} \kappa_n \frac{s^n}{n!}. \quad (11)$$

The coefficients κ_n in the expansion are known as the cumulants of the random variable X . The first four order

cumulants κ_n are as follows:

$$\kappa_1(X) = \langle X \rangle, \text{(Mean)} \quad (12)$$

$$\kappa_2(X) = \mu_2(X), \text{(Variance)} \quad (13)$$

$$\kappa_3(X) = \mu_3(X), \text{(Skewness)} \quad (14)$$

$$\kappa_4(X) = \mu_4(X) - 3[\mu_2(X)]^2, \text{(Kurtosis)} \quad (15)$$

Here, the n -th order central moment $\mu_n(X)$ is defined as

$$\mu_n(X) = \langle (X - \langle X \rangle)^n \rangle. \quad (16)$$

Cumulants are fundamental descriptors of the statistical properties of a random variable. While moments $\{\mu_n\}$ mix correlations of various orders, cumulants κ_n isolate the pure, irreducible n -th order correlation structure, representing the part of the moment that cannot be explained by lower-order statistics. This property makes them indispensable in the study of correlations and non-Gaussianity.

B. Higher-order quantum correlations in bipartite system

Let $\mathcal{S} = \sum_{i,j} c_{ij} X_i \otimes Y_j$ be a joint measurement operator in a bipartite system with $c_{ij} \in \mathbb{C}$, then the statistical cumulant $\kappa_n(\mathcal{S})$ exists if the observables X_i, Y_j have the moments up to order n [32]. We present the following proposition:

Proposition 1. *A bipartite system exhibits n -th order quantum correlations if it violates the following inequality:*

$$m \leq \kappa_n(\mathcal{S}) \leq M, \quad (17)$$

where m and M are the lower and upper bounds of the n -th order cumulant $\kappa_n(\mathcal{S})$ imposed by classical theory.

As a demonstration of Proposition 1, we derive the generalized CH inequality from the nonnegativity of the second-order cumulant of the generalized CH operator \mathcal{B}_{CH} defined in Eq. (8). In any LHV theory, the measurement outcomes are predetermined by a hidden variable λ with distribution $\rho(\lambda)$. From Eq. (3), the classical expectation value of \mathcal{B}_{CH} , is given by:

$$\langle \mathcal{B}_{\text{CH}} \rangle_{\text{lhv}} = \int \mathcal{B}_{\text{CH}}(\lambda) \rho(\lambda) d\lambda, \quad (18)$$

where $\mathcal{B}_{\text{CH}}(\lambda)$ represents the deterministic value of the operator for a given λ .

The critical distinction between quantum and classical descriptions lies in the algebraic properties of the operator. In quantum mechanics, the non-commutativity of local observables (e.g., $[\boldsymbol{\sigma} \cdot \mathbf{a}, \boldsymbol{\sigma} \cdot \mathbf{a}'] \neq 0$) allows the operator to span a larger spectrum. In contrast, within any LHV model, all local observables commute. Then, from the nonnegativity of the second-order cumulant of \mathcal{B}_{CH} :

$$\kappa_2(\mathcal{B}_{\text{CH}}) \geq 0, \quad (19)$$

we have the following fundamental corollary (see Section A for details):

Corollary 1. *For any bipartite system composed of two subsystems A and B , if the joint probabilities $p_{jk}(\mathbf{a}, \mathbf{b})$ can be described by LHV theory, then the following inequalities hold:*

$$-|\alpha_a \alpha_b| \leq \langle \mathcal{B}_{\text{CH}} \rangle_{\text{lhv}} \leq 0. \quad (20)$$

Here $\alpha_{a,b}$ are bias and unsharpness parameters on A and B , defined in Eq. (8).

It is noteworthy that Eq. (20) reproduces the standard CH inequality [5] when $\alpha_a = \alpha_b = 1$ (i.e., projective measurements without bias). While most previous works use only the upper bound of Eq. (20) to test local realism, the lower bound is equally important in our analysis of higher-order quantum correlations.

As defined in Eq. (14), the third-order cumulant (skewness) of \mathcal{B}_{CH} is

$$\kappa_3(\mathcal{B}_{\text{CH}}) = \langle \mathcal{B}_{\text{CH}}^3 \rangle - 3\langle \mathcal{B}_{\text{CH}} \rangle \langle \mathcal{B}_{\text{CH}}^2 \rangle + 2\langle \mathcal{B}_{\text{CH}} \rangle^3. \quad (21)$$

The boundedness condition derived in Corollary 1 has profound implications for higher-order statistics. Exploiting the mathematical limits established for bounded random variables in [33], we have (see Section B for details):

Corollary 2. *For any bipartite system composed of two subsystems A and B , the local realism imposes the following constraint on the third-order cumulant of the CH operator:*

$$|\kappa_3(\mathcal{B}_{\text{CH}})| \leq \frac{|\alpha_a \alpha_b|^3}{8}, \quad (22)$$

Here, \mathcal{B}_{CH} is defined in Eq. (8).

Violation of this skewness bound indicates the higher-order quantum correlation in the system, which provides a rigorous witness even when the Eq. (20) holds.

IV. FORMALISM OF GENERALIZED POVM MEASUREMENT IN HYPERON DECAY

The weak decay of a hyperon Y (e.g., Λ, Σ^+) exhibits a parity-violating angular distribution given by [34]:

$$\frac{dN_Y}{d\Omega} = \frac{1}{4\pi} (1 + \alpha_Y \mathbf{P}_Y \cdot \mathbf{n}), \quad (23)$$

where \mathbf{P}_Y is the hyperon polarization vector, \mathbf{n} is the unit vector along the decay product's momentum, and α_Y is the weak decay parameter characterizing the asymmetry. In the helicity frame, where the z -axis aligns with the hyperon momentum and the y -axis is normal to the production plane, the probability of detecting the decay product along \mathbf{n} is

$$P_Y(\mathbf{n}) = \frac{1}{2} (1 + \alpha_Y |\mathbf{P}_Y| \cos \theta), \quad (24)$$

with θ denoting the angle between \mathbf{P}_Y and \mathbf{n} .

To interpret this process through quantum measurement theory, we formalize the weak decay as a generalized POVM on the hyperon spin [27], extending the framework to mixed states. Without loss of generality, the decay $\Lambda \rightarrow p\pi^-$ serves as a representative example. With the initial Λ spin state denoted by ρ_Λ and the momentum space initialized in the ground state $|\mathbf{g}_p\rangle$, the total initial state is given by:

$$\varrho_i = \rho_\Lambda \otimes |\mathbf{g}_p\rangle\langle\mathbf{g}_p| . \quad (25)$$

During the decay, the weak interaction operator U couples the spin and momentum Hilbert spaces, evolving the system to

$$\begin{aligned} \varrho_f &= U(\rho_\Lambda \otimes |\mathbf{g}_p\rangle\langle\mathbf{g}_p|)U^\dagger \\ &= \sum_{j,k \in \{+,-\}} (M_j(\mathbf{n}_p)\rho_\Lambda M_k^\dagger(\mathbf{n}_p)) \otimes |j\mathbf{n}_p\rangle\langle k\mathbf{n}_p| , \end{aligned} \quad (26)$$

where $|\mathbf{n}_p\rangle$ represents the proton momentum state. The Kraus operators $M_\pm(\mathbf{n}_p)$ are defined as

$$M_\pm(\mathbf{n}_p) = \frac{1}{2(|S|^2 + |P|^2)} (S \pm P \boldsymbol{\sigma} \cdot \mathbf{n}_p) , \quad (27)$$

with S and P being the s - and p -wave decay amplitudes. The asymmetry parameter is identified as $\alpha_\Lambda = \frac{2 \operatorname{Re}(S^* P)}{|S|^2 + |P|^2}$.

Tracing out the spin degrees of freedom yields the reduced density matrix for the proton:

$$\rho_p = \sum_{j,k \in \{+,-\}} \operatorname{Tr}[(M_j(\mathbf{n}_p)\rho_\Lambda M_k^\dagger(\mathbf{n}_p))] \otimes |j\mathbf{n}_p\rangle\langle k\mathbf{n}_p| . \quad (28)$$

Consequently, a projective measurement of the proton momentum along \mathbf{n}_p effectively implements a general POVM on the initial Λ spin state, described by the elements

$$E_\pm(\mathbf{n}_p) = \frac{1}{2} (I \pm \alpha_\Lambda \boldsymbol{\sigma} \cdot \mathbf{n}_p) , \quad (29)$$

which satisfy the completeness relation $\sum_\pm E_\pm(\mathbf{n}_p) = I$. Here, $E_\pm(\mathbf{n}_p) = M_\pm^\dagger(\mathbf{n}_p)M_\pm(\mathbf{n}_p)$. Accordingly, the probability of capturing the proton in the direction \mathbf{n}_p is predicted by quantum theory as

$$P_\pm(\mathbf{n}_p) = \operatorname{Tr}[\rho_\Lambda E_\pm(\mathbf{n}_p)] = \frac{1}{2}(1 \pm \alpha_\Lambda \mathbf{P}_\Lambda \cdot \mathbf{n}_p) . \quad (30)$$

Extending this to the joint decay of an entangled hyperon-antihyperon pair (e.g., $\Lambda \rightarrow p\pi^-$ and $\bar{\Lambda} \rightarrow \bar{p}\pi^+$), the joint probability of detecting the decay products along directions \mathbf{n}_p and $\mathbf{n}_{\bar{p}}$ is

$$P_{jk}(\mathbf{n}_p, \mathbf{n}_{\bar{p}}) = \operatorname{Tr}[\rho_{\Lambda\bar{\Lambda}} E_j(\mathbf{n}_p) \otimes E_k(\mathbf{n}_{\bar{p}})] , \quad (31)$$

where $j, k \in \{+,-\}$ and $\rho_{\Lambda\bar{\Lambda}}$ is the spin state of the entangled $\Lambda\bar{\Lambda}$ pair. This formalism is general and applies to

other hyperon decays, such as $\Sigma^+ \rightarrow p\pi^0$, by substituting the appropriate decay parameter α_Y .

Thus, hyperon weak decays provide a natural physical realization of general POVM measurements defined in Eq. (1) with bias $\eta = 0$ and unsharpness $|\alpha_Y| < 1$. Applying Corollary 1, we obtain the CH inequality for this system:

$$\begin{aligned} -|\alpha_Y \alpha_{\bar{Y}}| &\leq \mathbf{B}_{\text{CH}} \equiv P(\mathbf{n}_p, \mathbf{n}_{\bar{p}}) - P(\mathbf{n}_p, \mathbf{n}'_{\bar{p}}) + \\ &\quad P(\mathbf{n}'_p, \mathbf{n}_{\bar{p}}) + P(\mathbf{n}'_p, \mathbf{n}'_{\bar{p}}) - P(\mathbf{n}'_p) \\ &\quad - P(\mathbf{n}_{\bar{p}}) + \frac{1 - |\alpha_Y||\alpha_{\bar{Y}}|}{2} \leq 0 . \end{aligned} \quad (32)$$

It is noteworthy that a rigorous test of local realism demands independence from assumptions intrinsic to quantum theory. Consequently, in the analysis of bipartite $Y\bar{Y}$ systems, the renormalization of spin correlation functions via the decay asymmetry parameter α_Y constitutes a logical circularity. In contrast, the criterion formulated in Eq. (32) is constructed directly from measurement statistics, thereby circumventing this renormalization loophole.

In the subsequent analysis, we assume approximate CP conservation ($|\alpha_Y| = |\alpha_{\bar{Y}}|$). The relevant production and decay parameters for the $\chi_{c0}/\eta_c \rightarrow Y\bar{Y}$ and $J/\psi \rightarrow Y\bar{Y}$ processes are summarized in Table I.

V. TESTING HIGHER-ORDER QUANTUM CORRELATIONS WITH ENTANGLED HYPERON-ANTIHYPERON PAIRS

In this section, the higher-order cumulant criteria are tested in entangled hyperon-antihyperon systems.

A. Excluding the timelike background in experiments

A genuine Bell test requires the entangled hyperon pairs to be spacelike separated, which cannot be guaranteed for each pair of hyperons produced in high-energy experiments. The timelike events may introduce local correlations that could mimic nonlocal quantum correlations, potentially invalidating the Bell test. Fortunately, one can obtain the fraction of space-like separation events over the total events. For a specific decay event, given the distances x_1 and x_2 traveled by the hyperon and anti-hyperon before decay, respectively, the condition for spacelike separation (in the rest frame of the mother particle) is:

$$\frac{1}{k} \leq \frac{x_1}{x_2} \leq k . \quad (33)$$

Here $k = \frac{1+\beta_Y}{1-\beta_Y}$ and $\beta_Y = \frac{v_Y}{c}$ with v_Y being the velocity of hyperon Y and c the speed of light. The fraction of

TABLE I. Summary of physical parameters for charmonium decays into ground-state octet hyperon pairs used in numerical simulations. The table lists: (1) “Hyperon Decay” parameters including decay mode, asymmetry α_Y , and branching fraction \mathcal{B}_{dec} ; (2) “Hyperon Velocity (β)” for parent particles $\eta_c, \chi_{c0}, J/\psi$, calculated from Particle Data Group masses [35]; and (3) “ J/ψ Production Dynamics” parameters, including branching fractions, polarization parameters, and corresponding references. \mathcal{B}_{prod} is in units of 10^{-4} and \mathcal{B}_{dec} in %.

Hyperon Decay Process				Hyperon Velocity (β)			J/ ψ Production Dynamics			
Channel	Mode	α_Y	\mathcal{B}_{dec} (%)	η_c	χ_{c0}	J/ψ	\mathcal{B}_{prod} (10^{-4})	α_ψ	$\Delta\Phi$ (rad)	Refs
$\Lambda\bar{\Lambda}$	$\Lambda \rightarrow p\pi^-$	0.755(3)	64	0.664	0.757	0.693	19.43(33)	0.475(4)	0.752(8)	[36–39]
$\Sigma^+\bar{\Sigma}^-$	$\Sigma^+ \rightarrow p\pi^0$	-0.994(4)	52	0.604	0.718	0.640	15.0(24)	-0.508(7)	-0.270(15)	[40, 41]
$\Xi^-\bar{\Xi}^+$	$\Xi^- \rightarrow \Lambda\pi^-$	-0.379(4)	100	0.464	0.633	0.521	9.7(8)	0.586(16)	1.213(49)	[37, 42]
$\Xi^0\bar{\Xi}^0$	$\Xi^0 \rightarrow \Lambda\pi^0$	-0.375(3)	96	0.473	0.638	0.528	11.65(4)	0.514(16)	1.168(26)	[42–44]

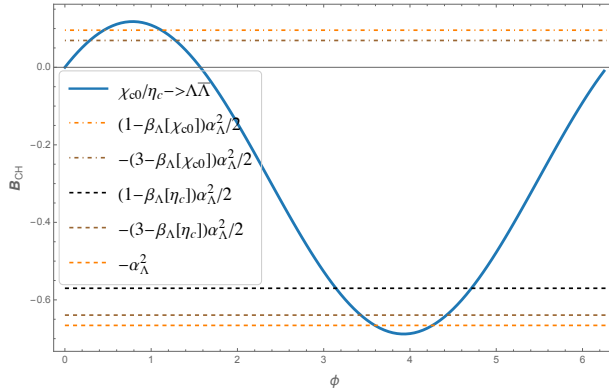


FIG. 1. Violation of the modified CH inequality Eq. (38) for the process $\chi_{c0}/\eta_c \rightarrow \Lambda\bar{\Lambda}$. The solid blue curve represents the quantum mechanical prediction for the spin-singlet state. The horizontal brown dot-dashed and dashed lines correspond to the upper and lower bounds in Eq. (38) for χ_{c0} , while the orange dot-dashed and dashed lines correspond to η_c . The black dashed line symbolizes the classical lower bound $(-\alpha_\Lambda^2)$ in Corollary 1.

spacelike separation events is given by [17]

$$f_s = \int_0^\infty e^{-x_2} dx_2 \int_{\frac{x_2}{k}}^{kx_2} e^{-x_1} dx_1 = \frac{k-1}{k+1} = \beta_Y. \quad (34)$$

While the joint probabilities of spacelike separated events must satisfy Eq. (32) for local realism, i.e., upper bounded by zero, the timelike events may violate the inequality due to possible classical communication. Therefore, new bounds are needed.

As for the timelike events, the \mathbf{B}_{CH} in Eq. (32) may reach its extreme values, that is,

$$\max[\mathbf{B}_{CH}] = \frac{\alpha_Y^2}{2}, \quad \text{or} \quad \min[\mathbf{B}_{CH}] = -\frac{3\alpha_Y^2}{2} \quad (35)$$

By considering the fraction of spacelike separation events β_Y , the modified upper and lower bounds of Eq. (32) that accounts for the timelike background maybe respectively

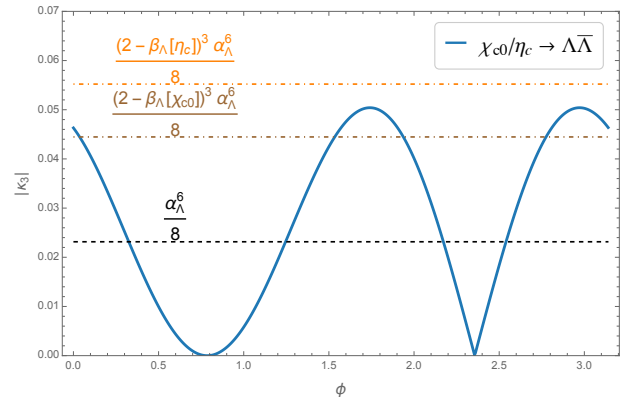


FIG. 2. Violation of the third-order cumulant criteria from Corollary 2 and Corollary 3 for the processes $\chi_{c0}/\eta_c \rightarrow \Lambda\bar{\Lambda}$. The solid blue curve represent the quantum prediction for the spin-singlet state in χ_{c0}/η_c decay. The horizontal orange and brown dot-dashed line symbolize the upper bounds in Corollary 3 for η_c and χ_{c0} channels, respectively. The black dashed line indicates the classical upper bound defined in Corollary 2.

given by

$$\beta_Y \cdot 0 + (1 - \beta_Y) \cdot \frac{\alpha_Y^2}{2} = (1 - \beta_Y) \frac{\alpha_Y^2}{2}, \quad (36)$$

$$\beta_Y \cdot (-\alpha_Y^2) + (1 - \beta_Y) \cdot \left(-\frac{3\alpha_Y^2}{2} \right) = - (3 - \beta_Y) \frac{\alpha_Y^2}{2}. \quad (37)$$

Then, we have the modified CH inequality as [27]

$$- (3 - \beta_Y) \frac{\alpha_Y^2}{2} \leq \mathbf{B}_{CH} \leq (1 - \beta_Y) \frac{\alpha_Y^2}{2}. \quad (38)$$

This leads to a corresponding restriction for the third-order cumulant of \mathbf{B}_{CH} :

Corollary 3. *For a bipartite system, taking into account the fraction β of spacelike separated events, local realism*

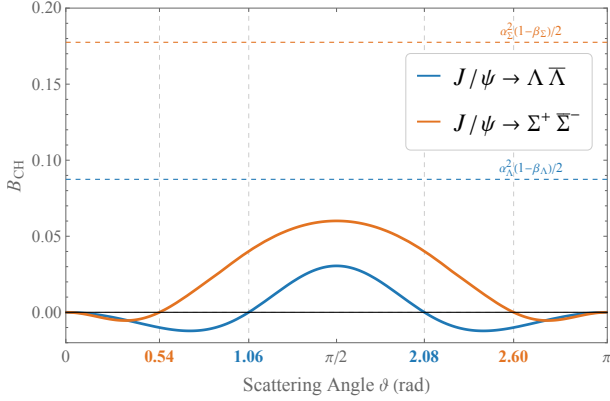


FIG. 3. Maximum value of $\langle \mathcal{B}_{\text{CH}} \rangle$ versus scattering angle ϑ for $\Lambda\bar{\Lambda}$ (blue solid) and $\Sigma^+\bar{\Sigma}^-$ (brown solid) in J/ψ decays. The classical upper bound (0) in Eq. (32) is marked by the black line, while the modified upper bounds defined in Eq. (38) are shown as dashed lines. Although the quantum predictions violate the former bound, they remain within the modified bounds across the entire range in terms of scattering angle.

imposes the following constraint on the third-order cumulant of the CH operator:

$$|\kappa_3(\mathcal{B}_{\text{CH}})| \leq \frac{(2-\beta)^3 \alpha^6}{8} . \quad (39)$$

B. $\chi_{c0}/\eta_c \rightarrow \Lambda\bar{\Lambda}$

For the process $\chi_{c0}/\eta_c \rightarrow \Lambda\bar{\Lambda}$, the spin state of the entangled $\Lambda\bar{\Lambda}$ pair is characterized by singlet state

$$|\psi_s\rangle = \frac{1}{\sqrt{2}}(|+-\rangle - |--\rangle) . \quad (40)$$

By adopting the measurement configuration as follows:

$$\begin{aligned} \mathbf{n}_p &= (1, 0, 0) , & \mathbf{n}'_p &= (0, 1, 0) , \\ \mathbf{n}_{\bar{p}} &= (\cos \phi, \sin \phi, 0) , & \mathbf{n}'_{\bar{p}} &= (-\sin \phi, \cos \phi, 0) , \end{aligned} \quad (41)$$

the quantum prediction for the CH quantity is

$$\mathbf{B}_{\text{CH}} = \langle \mathcal{B}_{\text{CH}} \rangle = \frac{\alpha_\Lambda^2}{2} (\cos \phi + \sin \phi - 1) . \quad (42)$$

The maximum value of \mathbf{B}_{CH} is $\frac{\alpha_\Lambda^2}{2}(\sqrt{2}-1)$, which occurs at $\phi = \frac{\pi}{4}$. Thus, the violation of the modified CH inequality in Eq. (38) requires $\beta_\Lambda > 2 - \sqrt{2} \approx 0.586$. Since the spacelike fractions for χ_{c0} ($\beta_\Lambda[\chi_{c0}] \approx 0.757$) and η_c ($\beta_\Lambda[\eta_c] \approx 0.664$) both exceed this threshold, the two processes can successfully demonstrate nonlocality via the generalized CH inequality see Fig. 1.

Using the same measurement settings in Eq. (41), the skewness function is derived as:

$$\kappa_3^{(\chi/\eta)} = -\frac{\sqrt{2}}{8} \alpha_\Lambda^6 \left[\sin \left(\phi + \frac{\pi}{4} \right) - \sin \left(3\phi - \frac{\pi}{4} \right) \right] , \quad (43)$$

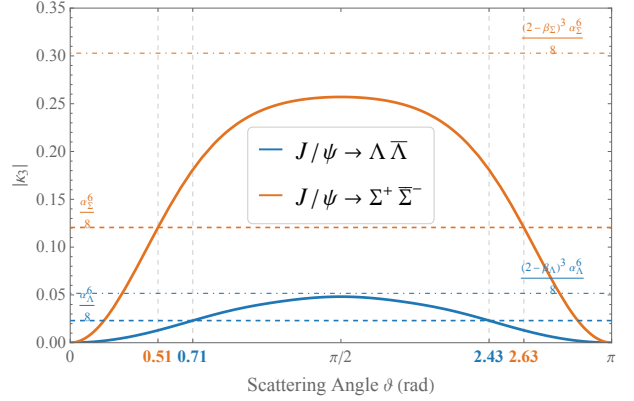


FIG. 4. Third-order cumulant $|\kappa_3(\mathcal{B}_{\text{CH}})|$ versus scattering angle ϑ for entangled $\Sigma^+\bar{\Sigma}^-$ and $\Lambda\bar{\Lambda}$ pairs produced in J/ψ decays. The solid blue and brown curves represent the quantum predictions for $\Lambda\bar{\Lambda}$ and $\Sigma^+\bar{\Sigma}^-$, respectively. The horizontal dot-dashed lines indicate the modified upper bounds from Corollary 3, while the dashed lines represent the upper bounds defined in Corollary 2 for $\Lambda\bar{\Lambda}$ (orange) and $\Sigma^+\bar{\Sigma}^-$ (brown).

which achieves its maximum value of $\frac{\sqrt{6}}{9} \alpha_\Lambda^6$ at $\arcsin\left(\frac{1}{\sqrt{3}}\right) - \frac{\pi}{4}$. The critical velocity threshold for the violation of the bound in Corollary 3 is $\beta_c = 2 - \sqrt[3]{8\sqrt{6}/9} \approx 0.704$.

As illustrated in Fig. 2, the inequality in Eq. (22) is violated over a wide range of the parameter ϕ . This indicates that the correlation terms in \mathcal{B}_{CH} induce a skewness significantly higher than classically admissible, reflecting the presence of higher-order dependencies. Although both the $\chi_{c0} \rightarrow \Lambda\bar{\Lambda}$ and $\eta_c \rightarrow \Lambda\bar{\Lambda}$ processes violate the bound derived in Corollary 2, only the violation in the χ_{c0} channel persists under the modified bound given in Corollary 3.

C. $J/\psi \rightarrow Y\bar{Y}$

In the BESIII experiment, large samples of entangled hyperon-antihyperon pairs are produced via J/ψ decays. The spin state of the entangled $Y\bar{Y}$ pair is described by the general two-qubit density matrix:

$$\begin{aligned} \rho_{Y\bar{Y}} = & \frac{1}{4} [I \otimes I + \mathbf{P}_Y \cdot \boldsymbol{\sigma} \otimes I + I \otimes \mathbf{P}_{\bar{Y}} \cdot \boldsymbol{\sigma} \\ & + \sum_{i,j} C_{ij} \sigma_i \otimes \sigma_j] . \end{aligned} \quad (44)$$

Through local unitary operations [45, 46], this state can be transformed into the standard symmetric two-qubit X-state:

$$\rho_{Y\bar{Y}} = \frac{1}{4} [I \otimes I + a\sigma_z \otimes I + I \otimes a\sigma_z + \sum_i t_i \sigma_i \otimes \sigma_i] . \quad (45)$$

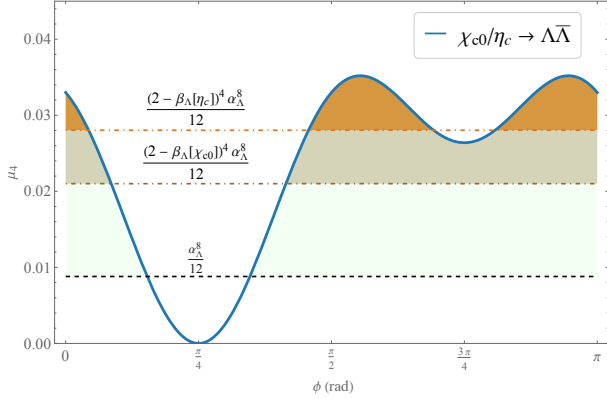


FIG. 5. Fourth-order central moment μ_4 versus scanning angle ϕ for $\chi_{c0}/\eta_c \rightarrow \Lambda\bar{\Lambda}$ decays. The quantum prediction is shown as a solid blue curve. The classical bound from Eq. (57) is indicated by the black dashed line, while the timelike-modified bounds from Eq. (58) for χ_{c0} and η_c are depicted by dot-dashed lines. Shaded regions highlight the violations of these classical limits.

The coefficients are determined by the decay kinematics:

$$a = |\mathbf{P}_Y| = \frac{\gamma_\psi \sin \vartheta \cos \vartheta}{1 + \alpha_\psi \cos^2 \vartheta}, \quad (46)$$

$$t_{1,2} = \frac{1 + \alpha_\psi \pm \sqrt{(1 + \alpha_\psi \cos 2\vartheta)^2 - \gamma_\psi^2 \sin^2 2\vartheta}}{2(1 + \alpha_\psi \cos^2 \vartheta)}, \quad (47)$$

$$t_3 = \frac{-\alpha_\psi \sin^2 \vartheta}{1 + \alpha_\psi \cos^2 \vartheta}, \quad (48)$$

where $\gamma_\psi = \sqrt{1 - \alpha_\psi^2} \sin \Delta\Phi$. Here, $\alpha_\psi \in [-1, 1]$ is the decay parameter of the vector charmonium ψ , $\Delta\Phi \in (-\pi, \pi]$ represents the relative phase of the form factors, and ϑ denotes the scattering angle of the hyperon Y in the J/ψ rest frame. The explicit values of α_ψ and $\Delta\Phi$ for various $J/\psi \rightarrow Y\bar{Y}$ channels are listed in Table I.

For entangled hyperon-antihyperon pairs $Y\bar{Y}$ produced in J/ψ decays, the maximal expectation value of the CHSH operator is given by [47]:

$$2\sqrt{\lambda_1 + \lambda_2}, \quad (49)$$

where λ_1 and λ_2 ($\lambda_i \leq 1$) denote the two largest eigenvalues of the correlation matrix $T = \text{diag}(t_1, t_2, t_3)$. Correspondingly, the expectation value of the generalized CH operator \mathcal{B}_{CH} (defined in Eq. (8)) is bounded by the quantum mechanical limits:

$$-\frac{\alpha_Y^2 \sqrt{\lambda_1 + \lambda_2}}{2} - \frac{1}{2} \alpha_Y^2 \leq \langle \mathcal{B}_{\text{CH}} \rangle \leq \frac{\alpha_Y^2 \sqrt{\lambda_1 + \lambda_2}}{2} - \frac{1}{2} \alpha_Y^2. \quad (50)$$

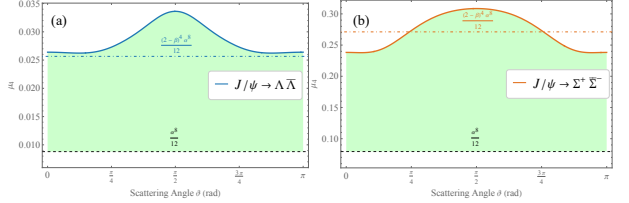


FIG. 6. The fourth-order central moment μ_4 as a function of the scattering angle ϑ for entangled hyperon pairs produced in J/ψ decay. (a) The results for the $\Sigma^+\bar{\Sigma}^-$ pair. The solid blue curve represents the quantum prediction, while the blue dot-dashed line denotes the modified upper bound derived in Eq. (58). (b) The results for the $\Lambda\bar{\Lambda}$ pair. The solid orange curve represents the quantum prediction, and the orange dot-dashed line denotes the modified upper bound. In both panels, the black dashed lines indicate the ideal classical upper bound from Eq. (57).

Violations of the bounds in Eq. (50) occur when:

$$\frac{\alpha_Y^2 \sqrt{\lambda_1 + \lambda_2}}{2} - \frac{1}{2} \alpha_Y^2 > (1 - \beta_Y) \frac{\alpha_Y^2}{2}, \quad (51)$$

$$-\frac{\alpha_Y^2 \sqrt{\lambda_1 + \lambda_2}}{2} - \frac{1}{2} \alpha_Y^2 < -(3 - \beta_Y) \frac{\alpha_Y^2}{2}. \quad (52)$$

The quantum predicted value $\langle \mathcal{B}_{\text{CH}} \rangle$ depends on the scattering angle ϑ , attaining its maximal values at $\vartheta = \pi/2$:

$$\frac{\alpha_Y^2 \sqrt{1 + \alpha_\psi^2}}{2} - \frac{1}{2} \alpha_Y^2. \quad (53)$$

Therefore, violating the modified upper bound in Eq. (36) requires the following kinematic condition:

$$\beta_Y + \sqrt{1 + \alpha_\psi^2} - 2 > 0. \quad (54)$$

In the relativistic limit $\beta_Y \rightarrow 1$, the CH inequalities in Eq. (32) would indeed be violated by the hyperon pairs from J/ψ decay. However, for the relevant hyperon channels ($Y = \Lambda, \Sigma^+, \Xi^0, \Xi^-$), this condition remains unsatisfied due to the moderate hyperon velocities β_Y and the small magnitude of the decay parameter α_ψ . This is illustrated in Fig. 3, where the left-hand side of Eq. (51) is plotted against ϑ for entangled $\Sigma^+\bar{\Sigma}^-$ and $\Lambda\bar{\Lambda}$ pairs. The numerical results confirm that the modified upper bound in Eq. (38) is respected across the entire ϑ range.

To investigate higher-order correlations in J/ψ decay processes, let us consider the measurement settings defined by the directions:

$$\mathbf{n}_p = (0, 0, 1), \quad \mathbf{n}'_p = (0, 1, 0), \\ \mathbf{n}_{\bar{p}} = \frac{1}{\sqrt{2}}(0, 1, -1), \quad \mathbf{n}'_{\bar{p}} = \frac{1}{\sqrt{2}}(0, 1, 1). \quad (55)$$

Accordingly, this measurement setting gives the magnitude of third-order cumulant for the state in Eq. (45):

$$|\kappa_3^{(\psi)}| = \frac{\sqrt{2}\alpha_Y^6}{16} |(t_2 - t_3)((t_2 - t_3)^2 - 3t_1 - 1)|, \quad (56)$$

The third-order cumulants $\kappa_3^{(\psi)}$ for entangled $\Sigma^+\bar{\Sigma}^-$ and $\Lambda\bar{\Lambda}$ pairs are presented in Fig. 4 as functions of ϑ . Evidently, $\kappa_3^{(\psi)}$ violates the classical upper bound derived in Corollary 2 within certain scattering angle ranges, exhibiting higher-order quantum correlations. However, when accounting for the timelike modification, neither channel violates the stricter bound from Corollary 3, as depicted in Fig. 4.

Crucially, comparing Figs. 3 and 4 demonstrates that the violation windows (in terms of ϑ) for both $\Sigma^+\bar{\Sigma}^-$ and $\Lambda\bar{\Lambda}$ pairs are wider for the third-order cumulant in Corollary 2 than for the CH inequality in Eq. (32). This expanded range suggests that the third-order cumulant, as a higher-order statistical measure, is more sensitive to the non-linear quantum correlations.

D. The fourth-order central moment

While the first three cumulants correspond directly to moments or central moments (representing the mean, variance, and skewness, respectively), higher-order cumulants ($n \geq 4$) define a more complex algebraic structure involving polynomial combinations of moments. The fourth-order cumulant is the first instance where this distinction becomes significant. Despite their theoretical importance, deriving tight bounds for higher-order cumulants remains a nontrivial mathematical challenge [48–50].

Instead, we investigate the fourth-order central moment rather than the cumulant, which may provide useful insights of contextuality. Based on the constraints of bounded random variables [33], we have:

Corollary 4. *For any bipartite system, local realism imposes the following constraint on the fourth-order central moment of the CH operator:*

$$\mu_4(\mathcal{B}_{\text{CH}}) \leq \frac{\alpha^8}{12}. \quad (57)$$

Accounting for the fraction β of spacelike separated events, the modified upper bound becomes:

$$\mu_4(\mathcal{B}_{\text{CH}}) \leq \frac{(2-\beta)^4 \alpha^8}{12}. \quad (58)$$

Adopting the measurement settings defined in Eq. (41), the analytical expression for the fourth-order central moment of \mathcal{B}_{CH} for $\chi_{c0}/\eta_c \rightarrow \Lambda\bar{\Lambda}$ is derived as:

$$\mu_4^{(\chi/\eta)} = \frac{\alpha_\Lambda^8}{16} [2 - 2 \sin(2\phi) + 3 \cos^2(2\phi)], \quad (59)$$

which achieves its maximum value when $\sin(2\phi) = -\frac{1}{3}$. As illustrated in Fig. 5, the quantum prediction for μ_4 significantly exceeds both the classical limit in Eq. (57) and the stricter timelike-modified bound in Eq. (58) for both χ_{c0} and η_c channels.

Turning to the entangled hyperon-antihyperon pairs produced in J/ψ decay, and using the measurement settings in Eq. (55), the fourth-order central moment of \mathcal{B}_{CH} is given by

$$\mu_4^{(\psi)} = \frac{\alpha_\Lambda^8}{64} [-3(t_2 - t_3)^4 + 4(3t_1 - 1)(t_2 - t_3)^2 + 8(1 + t_1)]. \quad (60)$$

The $\mu_4^{(\psi)}$ for $\Lambda\bar{\Lambda}$ and $\Sigma^+\bar{\Sigma}^-$ pairs are numerically evaluated and depicted in Fig. 6 as functions of the scattering angle ϑ . Remarkably, it is observed that μ_4 violates the classical upper bound in Eq. (57) across the entire range of scattering angles ϑ .

For simplicity, let us consider the CHSH operator composed with the orthogonal measurement configuration $(\mathbf{n}_p \perp \mathbf{n}'_p, \mathbf{n}_{\bar{p}} \perp \mathbf{n}'_{\bar{p}})$, i.e.,

$$\mathcal{B}_{\text{CHSH}} = \mathbf{n}_p \cdot \boldsymbol{\sigma} \otimes (\mathbf{n}_{\bar{p}} + \mathbf{n}'_{\bar{p}}) \cdot \boldsymbol{\sigma} + \mathbf{n}'_p \cdot \boldsymbol{\sigma} \otimes (\mathbf{n}_{\bar{p}} - \mathbf{n}'_{\bar{p}}) \cdot \boldsymbol{\sigma}. \quad (61)$$

In the fourth-order central moment of $\mathcal{B}_{\text{CHSH}}$, the leading term is given by

$$\begin{aligned} \mathcal{B}_{\text{CHSH}}^4 = & 16I \otimes I + [\mathbf{n}_p \cdot \boldsymbol{\sigma}, \mathbf{n}'_p \cdot \boldsymbol{\sigma}]^2 \otimes [\mathbf{n}_{\bar{p}} \cdot \boldsymbol{\sigma}, \mathbf{n}'_{\bar{p}} \cdot \boldsymbol{\sigma}]^2 \\ & + 8[\mathbf{n}_p \cdot \boldsymbol{\sigma}, \mathbf{n}'_p \cdot \boldsymbol{\sigma}] \otimes [\mathbf{n}_{\bar{p}} \cdot \boldsymbol{\sigma}, \mathbf{n}'_{\bar{p}} \cdot \boldsymbol{\sigma}]. \end{aligned} \quad (62)$$

Recent studies suggest that non-trivial expectation values of squared commutators serve as signatures of state-independent contextuality [29], which may explain the full-range violation of the ideal upper bound in Eq. (57) by the fourth-order central moment for the entangled hyperon-antihyperon pairs produced in J/ψ decay as shown in Fig. 6. To clarify the exact role of the fourth-order central moment in revealing contextuality, further investigations are required, which we leave for future work.

E. Dynamical Origin of Correlations: Electromagnetic Form Factors

In the preceding sections, the parameters characterizing the quantum state $(\alpha_\psi, \Delta\Phi)$ and the kinematic threshold (β) were treated as phenomenological inputs derived from experiment. To fundamentally understand the conditions required to observe high-order nonlocality violations, we must examine the interplay between the underlying QCD dynamics and the kinematic regime of the collider.

From Eqs. (53) and (56), it is evident that the potential for violating local realism through both the CH inequality and high-order cumulants is intrinsically linked to the eigenvalues of the correlation matrix T , which are functions of the decay parameters α_ψ and $\Delta\Phi$. For the process $e^+e^- \rightarrow J/\psi \rightarrow Y\bar{Y}$, the spin correlations are dictated by the interference between the magnetic (G_M^ψ) and electric (G_E^ψ) form factors. The decay parameter α_ψ ,

which determines the weight of the entangled components in the density matrix, is related to the form factors by [51]:

$$\alpha_\psi = \frac{s|G_M^\psi|^2 - 4M^2|G_E^\psi|^2}{s|G_M^\psi|^2 + 4M^2|G_E^\psi|^2}, \quad (63)$$

where \sqrt{s} is the center-of-mass energy and M is the baryon mass. This relationship maps the continuous parameter space of form factors onto the observable correlation strength.

Two extreme dynamical regimes yield maximal entanglement, ideal for testing local realism. In the magnetic dominance limit ($|G_E^\psi| \rightarrow 0$), $\alpha_\psi \rightarrow 1$, preserving helicity. Conversely, in the electric dominance limit ($|G_M^\psi| \rightarrow 0$), $\alpha_\psi \rightarrow -1$. Both extremes correspond to maximally entangled spin states. However, experimental data (see Table 1) indicates that many hyperon channels, such as $J/\psi \rightarrow \Sigma^+ \bar{\Sigma}^-$, lie in a “mixed” regime where $\alpha_\psi \approx -0.508$. This interference between electric and magnetic amplitudes induces a deviation from the maximally entangled state. Furthermore, the relative phase $\Delta\Phi$ generates a transverse polarization P_y . This introduces single-particle terms into the density matrix that deviate from the Bell diagonal state structure, thereby explicitly reducing the entanglement concurrence below the limit set by α_ψ alone [46].

VI. CONCLUSIONS

In summary, addressing the unexplored regime beyond linear statistical moments, the higher-order quantum correlations are investigated in entangled hyperon-antihyperon systems via statistical cumulants of the generalized Clauser-Horne operator. A generalized CH inequality based on the second-order cumulant is formulated, and further extended to derive a rigorous third-order skewness bound.

The numerical analysis reveals distinct violation patterns. Specifically, the $\chi_{c0} \rightarrow \Lambda \bar{\Lambda}$ process exhibits a pronounced violation of the skewness constraint, surpassing the classical limit by a clear margin. Notably, this violation is shown to be robust against the kinematic contamination from timelike separated events, confirming that the higher-order quantum correlation in this channel is observable in high-energy experiments such as BE-SIII and Belle II. Crucially, for the spin-singlet states in η_c and χ_{c0} decays, the optimal kinematic configurations maximizing this third-order violation differ from those of the generalized CH inequality, demonstrating that higher-order statistics offer complementary sensitivity to quantum correlations.

Furthermore, the $J/\psi \rightarrow \Sigma^+ \bar{\Sigma}^-$ and $\Lambda \bar{\Lambda}$ processes violate the third-order cumulant criterion with a strictly wider window in terms of the scattering angle compared to the generalized CH inequality. However, when incorporating the timelike modification, neither channel vio-

lates the stricter generalized CH inequality or the modified third-order bound. Moreover, the exploration of the fourth-order central moment shows that it exceeds the classical limit across the entire scattering angle range for hyperon pairs from J/ψ decay, suggesting a potential link to state-independent contextuality.

Finally, the dynamical origins of these correlations are analyzed in terms of electromagnetic form factors. It is found that the interference between electric and magnetic form factors leads to a departure from maximal entanglement. This insight underscores the intricate interplay between QCD dynamics and quantum correlations in hadronic systems.

ACKNOWLEDGEMENTS

This work was supported in part by National Natural Science Foundation of China (NSFC) under the Grants 12475087 and 12235008, and University of Chinese Academy of Sciences.

Appendix A: Proof of Lemma 1

The generalized CH operator is defined as

$$\begin{aligned} \mathcal{B}_{\text{CH}} \equiv & E_+(\mathbf{a}) \otimes E_+(\mathbf{b}) - E_+(\mathbf{a}) \otimes E_+(\mathbf{b}') \\ & + E_+(\mathbf{a}') \otimes E_+(\mathbf{b}) + E_+(\mathbf{a}') \otimes E_+(\mathbf{b}') \\ & - (1 + \eta_b) E_+(\mathbf{a}') \otimes I - (1 + \eta_a) I \otimes E_+(\mathbf{b}) \\ & + \frac{(1 + \eta_a)(1 + \eta_b) - |\alpha_a \alpha_b|}{2} I \otimes I. \end{aligned} \quad (A1)$$

Here, the general POVM operator $E_+(\mathbf{n})$ is given by

$$E_+(\mathbf{n}) = \frac{1}{2}(\xi + \alpha \mathbf{n} \cdot \boldsymbol{\sigma}), \quad (A2)$$

with $\boldsymbol{\sigma}$ is the vector of Pauli matrices.

The second-order cumulant of \mathcal{B}_{CH} is defined as follows

$$\kappa_2(\mathcal{B}_{\text{CH}}) = \langle \mathcal{B}_{\text{CH}}^2 \rangle - \langle \mathcal{B}_{\text{CH}} \rangle^2. \quad (A3)$$

First, it can be derived that the square of the CH operator defined in Eq. (8) satisfies the identity:

$$\mathcal{B}_{\text{CH}}^2 = -|\alpha_a \alpha_b| \mathcal{B}_{\text{CH}} - \alpha_a^2 \alpha_b^2 \mathcal{C}, \quad (A4)$$

where $\mathcal{C} = [\mathbf{a} \cdot \boldsymbol{\sigma}, \mathbf{a}' \cdot \boldsymbol{\sigma}] \otimes [\mathbf{b} \cdot \boldsymbol{\sigma}, \mathbf{b}' \cdot \boldsymbol{\sigma}] / 16$. Thus, the non-negativity of the second-order cumulant of \mathcal{B}_{CH} implies that

$$-|\alpha_a \alpha_b| \langle \mathcal{B}_{\text{CH}} \rangle - \langle \mathcal{B}_{\text{CH}} \rangle^2 - \alpha_a^2 \alpha_b^2 \langle \mathcal{C} \rangle \geq 0, \quad (A5)$$

In any LHV theory, there exists a joint distribution model for the four dichotomic observables and all local observables commute [31, 52], i.e., $\langle \mathcal{C} \rangle = 0$, which leads to

$$-|\alpha_a \alpha_b| \langle \mathcal{B}_{\text{CH}} \rangle_{\text{lhv}} - \langle \mathcal{B}_{\text{CH}} \rangle_{\text{lhv}}^2 \geq 0. \quad (A6)$$

By solving this inequality, one can obtain that $\langle \mathcal{B}_{\text{CH}} \rangle_{\text{lhv}}$ is strictly bounded in the interval:

$$\langle \mathcal{B}_{\text{CH}} \rangle_{\text{lhv}} \in [-|\alpha_a \alpha_b|, 0]. \quad (A7)$$

Appendix B: Proof of the upper bounds on high-order central moments

For any random variable X supported on a bounded interval $[A, B]$ of length $L = B - A$, the statistical cumulants are strictly constrained by the geometry of the support. The third-order cumulant (skewness), $\kappa_3 = \langle (X - \mu)^3 \rangle$, satisfies the algebraic inequality for bounded variables [33]:

$$|\kappa_3| \leq \frac{(B - A)^3}{8}. \quad (\text{B1})$$

Substituting the support length $L = |\alpha_a \alpha_b|$ derived from the LHV constraint, we obtain the necessary condition for local realism:

$$|\kappa_3(\mathcal{B}_{CH})| \leq \frac{|\alpha_a \alpha_b|^3}{8}. \quad (\text{B2})$$

This completes the proof of Corollary 2. The proof of Corollary 3 can be similarly established.

Similarly, for the fourth-order central moment $\mu_4 = \langle (X - \mu)^4 \rangle$, the upper bound for a random variable defined on an interval of length L is given by limits [33]:

$$\mu_4 \leq \frac{L^4}{12}. \quad (\text{B3})$$

Substituting $L = |\alpha_a \alpha_b|$ (and setting $|\alpha_a| = |\alpha_b| = \alpha$ for simplicity), we arrive at the bound:

$$\mu_4(\mathcal{B}_{CH}) \leq \frac{\alpha^8}{12}. \quad (\text{B4})$$

This completes the proof of Corollary 4.

[1] A. Einstein *et al.*, *Can quantum-mechanical description of physical reality be considered complete?* *Physical Review* **47**, 777 (1935).

[2] J. S. Bell, *On the Einstein Podolsky Rosen paradox*, *Physics Physique Fizika* **1**, 195–200 (1964).

[3] J. F. Clauser *et al.*, *Proposed experiment to test local hidden-variable theories*, *Physical Review Letters* **23**, 880–884 (1969).

[4] S. J. Freedman and J. F. Clauser, *Experimental test of local hidden-variable theories*, *Physical Review Letters* **28**, 938–941 (1972).

[5] J. F. Clauser and M. A. Horne, *Experimental consequences of objective local theories*, *Physical Review D* **10**, 526–535 (1974).

[6] A. Aspect *et al.*, *Experimental test of Bell's inequalities using time-varying analyzers*, *Physical Review Letters* **49**, 1804–1807 (1982).

[7] H. M. Wiseman *et al.*, *Steering, entanglement, nonlocality, and the Einstein-Podolsky-Rosen paradox*, *Phys Rev Lett* **98**, 140402 (2007).

[8] E. G. Cavalcanti *et al.*, *Experimental criteria for steering and the Einstein-Podolsky-Rosen paradox*, *Physical Review A* **80**, 032112 (2009).

[9] O. Gühne and G. Tóth, *Entanglement detection*, *Physics Reports* **474**, 1–75 (2009).

[10] R. Uola *et al.*, *Quantum steering*, *Reviews of Modern Physics* **92** (2020), 10.1103/RevModPhys.92.015001.

[11] N. Brunner *et al.*, *Bell nonlocality*, *Reviews of Modern Physics* **86**, 419–478 (2014).

[12] C. Branciard *et al.*, *Experimental falsification of Leggett's nonlocal variable model*, *Physical Review Letters* **99**, 210407 (2007).

[13] T. Paterek *et al.*, *Experimental test of nonlocal realistic theories without the rotational symmetry assumption*, *Physical Review Letters* **99**, 210406 (2007).

[14] S. Gröblacher *et al.*, *An experimental test of non-local realism*, *Nature* **446**, 871–875 (2007).

[15] C. Branciard *et al.*, *Testing quantum correlations versus single-particle properties within Leggett's model and beyond*, *Nature Physics* **4**, 681–685 (2008).

[16] C. Budroni *et al.*, *Kochen-Specker contextuality*, *Reviews of Modern Physics* **94**, 045007 (2022).

[17] N. A. Törnqvist, *Suggestion for einstein-podolsky-rosen experiments using reactions like $e^+e^- \rightarrow \lambda\bar{\lambda} \rightarrow \pi^-\pi^+\bar{p}$* , *Foundations of Physics* **11**, 171–177 (1981).

[18] J. Li and C.-F. Qiao, *Feasibility of testing local hidden variable theories in a charm factory*, *Physical Review D* **74**, 076003 (2006).

[19] J. Li and C.-F. Qiao, *New possibilities for testing local realism in high energy physics*, *Physics Letters A* **373**, 4311–4314 (2009).

[20] J. Li and C. Qiao, *Testing local realism in $P \rightarrow VV$ decays*, *Science China Physics, Mechanics and Astronomy* **53**, 870–875 (2010).

[21] Y. Shi and J.-C. Yang, *Entangled baryons: Violation of inequalities based on local realism assuming dependence of decays on hidden variables*, *The European Physical Journal C* **80**, 116 (2020).

[22] M. Fabbrichesi, R. Floreanini, and G. Panizzo, *Testing Bell inequalities at the lhc with top-quark pairs*, *Physical Review Letters* **127**, 161801 (2021).

[23] Y. Afik and J. R. M. de Nova, *Quantum discord and steering in top quarks at the lhc*, *Physical Review Letters* **130**, 221801 (2023).

[24] R. A. Bertlmann *et al.*, *Violation of a Bell inequality in particle physics experimentally verified?* *Physics Letters A* **332**, 355–360 (2004).

[25] A. Afriat and F. Selleri, *The Einstein, Podolsky, and Rosen Paradox in Atomic, Nuclear, and Particle Physics*, 1st ed. (Springer New York, NY, 2013) p. 248.

[26] B. C. Hiesmayr, *Limits of quantum information in weak interaction processes of hyperons*, *Scientific Reports* **5**, 11591 (2015).

[27] C. Qian *et al.*, *Nonlocal correlation of spin in high energy physics*, *Physical Review D* **101**, 116004 (2020).

[28] M. Ablikim *et al.*, *Test of local realism via entangled $\Lambda\bar{\Lambda}$ system*, *Nature Communications* **16**, 4948 (2025).

[29] M.-C. Yang, J.-L. Li, and C.-F. Qiao, *An effective way*

of characterizing the quantum nonlocality, *Quantum Information Processing* **22**, 242 (2023).

[30] B. S. Cirel'son, *Quantum generalizations of Bell's inequality*, *Letters in Mathematical Physics* **4**, 93–100 (1980).

[31] L. J. Landau, *On the violation of Bell's inequality in quantum theory*, *Physics Letters A* **120**, 54–56 (1987).

[32] A. Stuart and K. Ord, *Kendall's Advanced Theory of Statistics: Volume 1: Distribution Theory*, 6th ed., Vol. 1 (Wiley, 2010).

[33] M. Egozcue *et al.*, *The smallest upper bound for the pth absolute central moment of a class of random variables*, *Mathematical Scientist* **37**, 125 (2012).

[34] J. W. Cronin and O. E. Overseth, *Measurement of the decay parameters of the Λ^0 particle*, *Physical Review* **129**, 1795 (1963).

[35] S. Navas *et al.*, *Review of particle physics*, *Physical Review D* **110**, 030001 (2024).

[36] M. Ablikim *et al.* (BES Collaboration), *Polarization and entanglement in baryon–antibaryon pair production in electron–positron annihilation*, *Nature Physics* **15**, 631–634 (2019).

[37] M. Ablikim *et al.*, *Probing cp symmetry and weak phases with entangled double-strange baryons*, *Nature* **606**, 64–69 (2022).

[38] B. Collaboration *et al.*, *Study of J/Ψ and $\Psi(3686)$ decay to $\Lambda\bar{\Lambda}$ and $\Sigma^0\bar{\Sigma}^0$ final states*, *Physical Review D* **95**, 052003 (2017).

[39] B. Collaboration *et al.*, *Precise measurements of decay parameters and CP asymmetry with entangled Λ – $\bar{\Lambda}$ pairs*, *Physical Review Letters* **129**, 131801 (2022).

[40] B. Collaboration *et al.*, *First measurements of j/Ψ decays into $\Sigma^+\bar{\Sigma}^-$ and $\Xi^0\bar{\Xi}^0$* , *Physical Review D* **78**, 092005 (2008).

[41] B. Collaboration *et al.*, *Σ^+ and $\bar{\Sigma}^-$ polarization in the J/Ψ and $\Psi(3686)$ decays*, *Physical Review Letters* **125**, 052004 (2020).

[42] P. D. Group *et al.*, *Review of particle physics*, *Progress of Theoretical and Experimental Physics* **2022** (2022), 10.1093/ptep/ptac097.

[43] M. Ablikim *et al.*, *Study of J/ψ and $\psi(3686) \rightarrow \Sigma(1385)^0\bar{\Sigma}(1385)^0$ and $\Xi^0\bar{\Xi}^0$* , *Physics Letters B* **770**, 217–225 (2017).

[44] B. Collaboration *et al.*, *Tests of CP symmetry in entangled Ξ^0 – $\bar{\Xi}^0$ pairs*, *Physical Review D* **108**, L031106 (2023).

[45] T. Yu and J. H. Eberly, *Evolution from entanglement to decoherence of bipartite mixed "X" states*, *Quantum Information and Computation* **7**, 459 (2005).

[46] S. Wu *et al.*, *Bell Nonlocality and Entanglement in $E^+E^- \rightarrow Y\bar{Y}$ at BESIII*, *Physical Review D* **110**, 054012 (2024).

[47] R. Horodecki *et al.*, *Violating bell inequality by mixed spin-1/2 states: Necessary and sufficient condition*, *Physics Letters A* **200**, 340–344 (1995).

[48] Y. V. Prohorov and Y. A. Rozanov, *Probability Theory: Basic Concepts, Limit Theorems, Random Processes*, Vol. 18 (Springer, 1969).

[49] A. A. Dubkov and A. N. Malakhov, *Properties and interdependence of the cumulants of a random variable*, *Radiophysics and Quantum Electronics* **19**, 833–839 (1976).

[50] J. Zhang, *A universal moments-only bound for cumulants*, arXiv preprint arXiv:2510.05739 (2025).

[51] G. Fäldt and A. Kupsc, *Hadronic structure functions in the $e^+e^- \rightarrow \Lambda\bar{\Lambda}$ reaction*, *Physics Letters B* **772**, 16 (2017).

[52] A. Fine, *Hidden variables, joint probability, and the bell inequalities*, *Physical Review Letters* **48**, 291–295 (1982).